Long-Range Crystalline Nature of the Skyrmion Lattice in MnSi

T. Adams,[1] S. Mühlbauer,[1,2,3] C. Pfleiderer,[1] F. Jonietz,[1] A. Bauer,[1] A. Neubauer,[1] R. Georgii,[1,2] P. Böni,[1] U. Keiderling,[4] K. Everschor,[5] M. Garst,[5] and A. Rosch[5]

[1]*Physik-Department E21, Technische Universität München, D-85748 Garching, Germany*
[2]*Forschungsneutronenquelle Heinz Maier-Leibnitz, Technische Universität München, D-85748 Garching, Germany*
[3]*Institut für Festkörperphysik, ETH Zürich, Zürich, Switzerland*
[4]*Helmholtz Zentrum Berlin, BENSC, D-14109 Berlin, Germany*
[5]*Institute of Theoretical Physics, Universität zu Köln, D-50937 Köln, Germany*

(Received 5 July 2011; published 18 November 2011)

We report small angle neutron scattering of the Skyrmion lattice in MnSi using an experimental setup that minimizes the effects of demagnetizing fields and double scattering. Under these conditions, the Skyrmion lattice displays resolution-limited Gaussian rocking peaks that correspond to a magnetic correlation length in excess of several hundred micrometers. This is consistent with exceptionally well-defined long-range order. We further establish the existence of higher-order scattering, discriminating parasitic double scattering with Renninger scans. The field and temperature dependence of the higher-order scattering arises from an interference effect. It is characteristic for the long-range crystalline nature of the Skyrmion lattice as shown by simple mean-field calculations.

DOI: 10.1103/PhysRevLett.107.217206 PACS numbers: 75.10.−b, 75.25.−j, 75.50.−y

Single-crystal small angle neutron scattering (SANS) in the *A* phase of the itinerant helimagnet MnSi recently established a highly unusual sixfold symmetry of the scattering pattern perpendicular to the magnetic field **B** [1]. Regardless of the orientation of the crystal lattice with respect to the magnetic field, the same sixfold diffraction pattern was seen, characteristic of a magnetic structure which is almost completely decoupled from the underlying atomic lattice. A theoretical calculation in turn identified the *A* phase in MnSi as a Skyrmion lattice stabilized by thermal fluctuations, i.e., a new form of magnetic order composed of topologically stable knots in the spin structure. The associated nontrivial topology was confirmed by means of the topological Hall signal [2]. Both the theoretical analysis [1] and small angle neutron scattering in $Mn_{1-x}Fe_xSi$, $Mn_{1-x}Co_xSi$, and the strongly doped semiconductor $Fe_{1-x}Co_xSi$ further suggested that the Skyrmion lattice is a general phenomenon [3], with spin torque effects at ultralow current densities as the most spectacular property [4].

These studies inspired Lorentz force microscopy providing direct evidence of Skyrmion lattices and individual Skyrmions in $Fe_{1-x}Co_xSi$ [5], FeGe [6], and MnSi [7]. In the thin samples and for the perpendicular magnetic fields studied, the Skyrmion lattice is thereby more stable [5] than in the bulk, but with increasing sample thickness the magnetic phase diagram was found to approach that of bulk samples. This suggests that the same Skyrmion lattice is realized in bulk samples and thin films.

Taken together, a pressing question regarding the existence of Skyrmion lattices in bulk materials concerns direct microscopic evidence of their long-range crystalline nature, i.e., the precise spatial variation of the magnetization on very long scales. The quality of the long-range order strongly influences both the pinning forces [4,8] and the rotational spin torques in the presence of currents [4].

In principle, quantitative information on the magnetic structure can be obtained from a reconstruction from higher-order peaks in neutron scattering. However, previous neutron studies [1] were subject to strong double scattering, i.e., neutrons scattering twice from the magnetic structure, which are difficult to discern from higher-order peaks. Moreover, an exponential (rather than Gaussian) intensity variation of the rocking scans and streaks of intensity emanating radially from the first-order peaks [1] seemed to hint at unusual aspects of the morphology of the spin structure.

In this Letter, we report a high-resolution small angle neutron scattering study of pure MnSi to resolve these issues. As the Skyrmion lattice is extremely weakly coupled to the atomic lattice and follows closely the applied magnetic field, it is essential to guarantee a homogeneous magnetic field inside the sample by reducing all effects of demagnetization fields. We used therefore a thin sample with a thickness of ~1 mm which was illuminated in a small central section only. This also allowed us to reduce the amount of double scattering. Taking these precautions, we find sharp resolution-limited Gaussian rocking scans, while all peculiar features such as streaks of intensity vanished. Our results highlight that extreme care has to be exercised before claiming an unusual morphology of the Skyrmion lattice in any B20 compound.

As our main result we unambiguously establish higher-order scattering, by discriminating parasitic double scattering in Renninger scans. The magnetic field *B* and temperature *T* dependence of the higher-order scattering may thereby be quantitatively explained with an interference effect, providing unambiguous microscopic evidence of the long-range crystalline nature of the Skyrmion lattice in bulk samples of MnSi.

For our studies, two MnSi platelets denoted as samples *A* and *B* were cut from the same ingot used previously [1,4,9–11]. Sample *A* was $\sim 14 \times 9 \times 1.4$ mm^3, and sample *B* was $\sim 12 \times 7 \times 1$ mm^3, both with a crystalline $\langle 110 \rangle$ direction normal to the platelet. The crystalline mosaic spread was measured to be very small, $\sim 0.15°$. The specific heat and the resistivity of test pieces from the same ingot are in excellent agreement with the literature with a good residual resistivity ratio, ~ 100. The samples were prealigned by x-ray Laue backscattering. For precise alignment in the SANS studies at low T, we use that the magnetic structure at zero field is described by helices in $\langle 111 \rangle$ directions.

Our studies were carried out on the cold diffractometer MIRA at Munich and the SANS instrument V4 at Berlin. Neutrons with a wavelength $\lambda = 9.7$ Å $\pm$ 5% and $\lambda = 4.5$ Å $\pm$ 10% were used at MIRA and V4, respectively. The instrumental resolution at MIRA was $\Delta\beta_{az} = 4°$ in the azimuthal direction, $\Delta\beta_{\mathbf{q}} = 0.004$ Å^{-1} in the radial $|\mathbf{q}|$ direction, and $\Delta\beta_{\mathbf{k_f}} = 0.35°$ perpendicular to $|\mathbf{q}|$ in the direction of $\mathbf{k_f}$. This compares with a resolution of $\Delta\beta_{az} = 4.9°$, $\Delta\beta_{\mathbf{q}} = 0.003$ Å^{-1}, and $\Delta\beta_{\mathbf{k_f}} = 0.21°$ at V4. Temperatures are given with respect to the helimagnetic transition temperature T_c determined by SANS.

The importance of the sample thickness for SANS studies is evident from previous work in the helical state, where distinct double scattering was observed, e.g., Figs. 2(A) and 2(D) in Ref. [1]. Consistent with the entire literature on SANS in the zero field helical state (cf. Refs. [12,13], and references therein), typical data in the helical state of sample *A* (not shown) display a Gaussian rocking dependence with a rocking width of $\eta_m = 1.6°$ corresponding a correlation length $\sim 10^4$ Å. However, due to its reduced thickness, double scattering is strongly reduced in sample *A*.

The effects of the sample shape are most dramatic for SANS studies of the *A* phase as illustrated in Figs. 1(a) and 1(b), which reproduce Fig. 2(E) of Ref. [1]. These previous results suggested a rocking width similar to the helical state, with an unusual non-Gaussian line shape [Fig. 1(b)]. For another sample studied in Ref. [1], strong double scattering and even unexplained streaks of intensity emanating radially from the first-order scattering were seen. In stark contrast, we do not find any such peculiar features for our thin platelets [see Figs. 1(c) and 1(d)]. Moreover, the rocking dependence is now Gaussian with an extremely narrow width, $\eta_A = 0.45°$, slightly larger than the resolution limit $\Delta\beta_{\mathbf{k}f} = 0.35°$. Thus, the intrinsic magnetic correlation length of the Skyrmion lattice exceeds 100 μm and is therefore more than an order of magnitude larger than for the helical state. In contrast, previous studies reflected the

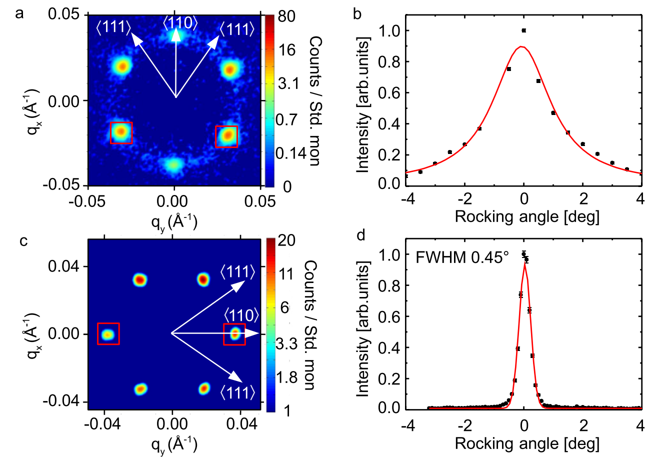

FIG. 1 (color online). Typical SANS data in the *A* phase of MnSi. (a) Intensity pattern in a thick cylindrical sample at $\mu_0 H = 0.16$ T as reported in Ref. [1]. (b) Rocking scan of the data shown in (a) as reported in Ref. [1]. (c) Intensity pattern in thin platelet (sample *A*) at $\mu_0 H = 0.2$ T. (d) Rocking scan of the data shown in (c); note the narrow Gaussian dependence.

variation of the internal magnetic field directions due to demagnetizing effects.

To distinguish double scattering from higher-order scattering, we used so-called Renninger scans depicted in Fig. 2(a) [14]. The sample is thereby first rotated together with the magnetic field around the vertical axis through an angle χ until the sum of two scattering vectors $\mathbf{q_1} + \mathbf{q_2}$

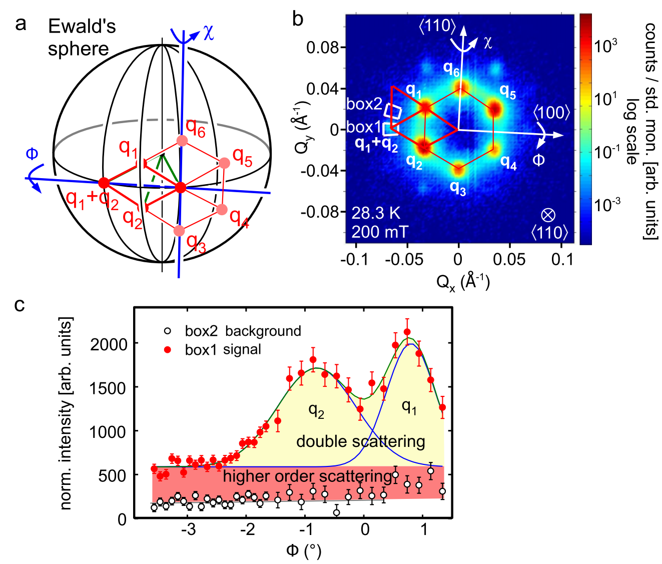

FIG. 2 (color online). Operating principle and typical data of Renninger scans at V4. (a) Ewald-sphere depiction of Renninger scans; see the text for details. (b) Typical scattering pattern obtained by a sum over a rocking scan around ϕ after background subtraction recorded at high T. (c) Intensity as a function of rocking angle ϕ in a Renninger scan. The intensity was integrated over the areas of boxes 1 and 2 in (b).

touches the Ewald sphere, thus satisfying the scattering condition. This is followed by the actual Renninger scan, which is a rocking scan with respect to $\mathbf{q_1} + \mathbf{q_2}$ through the angle ϕ, while recording the intensity at $\mathbf{q_1} + \mathbf{q_2}$. This way double scattering is ''rocked out'' of the scattering condition, while higher-order scattering continues to satisfy the scattering condition for all ϕ. For the Renninger scans sample B was mounted with its crystalline $\langle 110 \rangle$ direction parallel to the incoming neutron beam. A crystalline $\langle 100 \rangle$ direction was oriented approximately horizontally. The background was determined for T well above T_c for each rocking angle and subsequently subtracted. The intensity at $\mathbf{q_1} + \mathbf{q_2}$ as indicated by box 1 in Fig. 2(b) was then compared with the intensity in a box of equal size at a position slightly to the side of $\mathbf{q_1} + \mathbf{q_2}$, labeled box 2. Typical variations of the intensities in box 1 and box 2 with the angle ϕ are shown in Fig. 2(c) for $T = T_c - 0.5$ K and $\mu_0 H = 200$ mT. The intensity observed at $\mathbf{q_1} + \mathbf{q_2}$ clearly displays two contributions: (a) two Gaussian peaks due to double scattering when either $\mathbf{q_1}$ or $\mathbf{q_2}$ intersect the Ewald sphere and (b) a constant intensity arising due to true higher-order reflections (red shading).

Typical Renninger scans for $T = T_c - 0.5$ K and $T_c - 1.5$ K under magnetic fields of $\mu_0 H = 180$, 200, and 220 mT are shown in Fig. 3. With increasing T and B the higher-order scattering increases. The T and B dependence of the scattering intensities are summarized in Fig. 4. Figure 4(a) shows the field dependence of the first-order peaks at $\mathbf{q_1}$ and $T = T_c - 0.5$ K. The peak height is shown, which was confirmed to be proportional to the integrated intensity. Compared with the field dependence for $B \parallel \langle 111 \rangle$ reported in Ref. [15] for $T_c - 0.2$ K, we find a more gradual variation of the intensity. Figure 4(b) shows the ratio of the higher-order peak intensity at $\mathbf{q_1} + \mathbf{q_2}$ with respect to the first-order intensity at $\mathbf{q_1}$ for $T = T_c - 1.5$ K, $T_c - 1.0$ K, and $T_c - 0.5$ K. Above $\mu_0 H \approx 180$ mT, this ratio increases as a function of T and B. Unfortunately, it was not possible to track the higher-order scattering below $\mu_0 H = 180$ mT, since the first-order intensity was too weak.

In summary, our main experimental results are the following. (i) A strong magnetic field dependence of the second-order intensity, which appears to vanish for a certain field $B \approx B_{\rm int}$ inside the A phase. (ii) An increase of the second-order intensity with *increasing* T. This may seem counterintuitive, since the nonlinear effects leading to higher-order peaks should be less pronounced when all amplitudes decrease with increasing T. Finally, (iii) a tiny weight of the higher-order peaks of the order of 10^{-3}.

A complete quantitative theory of the Skyrmion phase requires account of the effects of thermal fluctuations [1]. Yet, a semiquantitative explanation of our experimental observations may already be obtained on the level of a mean-field approximation. After a rescaling of the

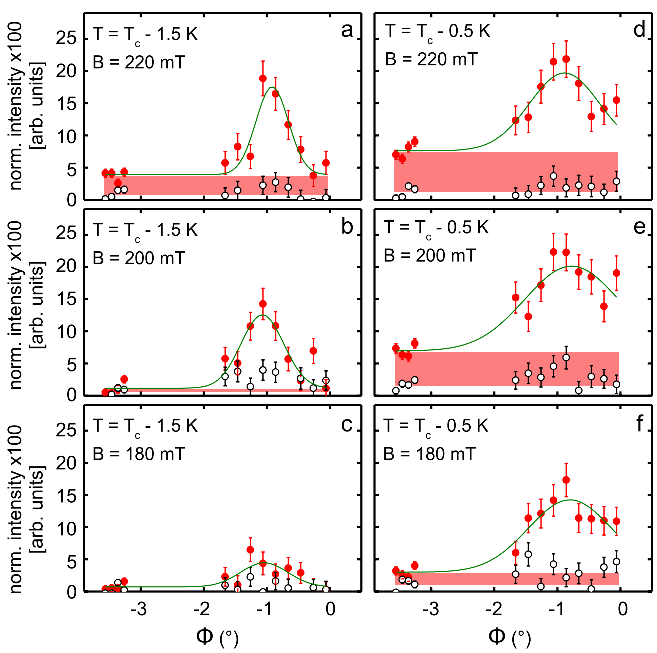

FIG. 3 (color online). Typical Renninger scans at various T and B in the A phase of MnSi. (a)–(c) were recorded at $T = T_c - 1.5$ K and magnetic fields $\mu_0 H = 180$, 200, and 220 mT, respectively. (d)–(f) show Renninger scans for $T = T_c - 0.5$ K and magnetic fields of $\mu_0 H = 180$, 200, and 220 mT, respectively. True higher-order scattering is shaded in red and remains constant for large ϕ.

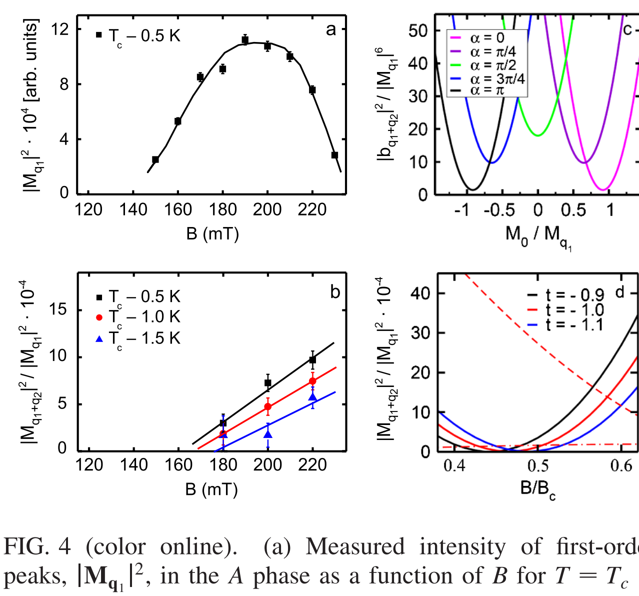

FIG. 4 (color online). (a) Measured intensity of first-order peaks, $|\mathbf{M}_{\mathbf{q}_1}|^2$, in the A phase as a function of B for $T = T_c - 0.5$ K. (b) Ratio of the intensity at $\mathbf{q_1} + \mathbf{q_2}$ and first-order diffraction at various temperatures. (c) Calculated staggered field at $|\mathbf{b}_{q_1+q_2}|^2$, Eq. (2), which induces the scattering at $\mathbf{q_1} + \mathbf{q_2}$ for different values of the phase α. (d) Calculated ratio of the higher-order diffraction at $\mathbf{q_1} + \mathbf{q_2}$ and first-order diffraction, $|M_{\mathbf{q}_1+\mathbf{q}_2}|^2/|M_{\mathbf{q}_1}|^2$ as a function of the magnetic field in mean-field theory for $t = -0.9$, -1, and -1.1 in the units of Eq. (1). Dashed (dot-dashed) line: $|M_{2\mathbf{q}_1}|^2/|M_{\mathbf{q}_1}|^2$ ($|M_{2\mathbf{q}_1+\mathbf{q}_2}|^2/|M_{\mathbf{q}_1}|^2$) for $t = -1$.

coordinates, magnetization, magnetic field, and free energy, the Ginzburg Landau free energy density in the presence of the Dzyaloshinskii-Moriya interaction $\sim\mathbf{M}(\nabla\times\mathbf{M})$ is given by [1,16,17]

$$F = (1+t)\mathbf{M}^2 + (\nabla\mathbf{M})^2 + 2\mathbf{M}(\nabla\times\mathbf{M}) + \mathbf{M}^4 - \mathbf{B}\mathbf{M}, \tag{1}$$

where t measures the distance to the $B=0$ mean-field critical temperature. Other contributions may be neglected, because they are higher order in spin-orbit coupling or result in small contributions close to the critical temperature where the Skyrmion lattice is stable. Minimizing F with the ansatz $\mathbf{M}(\mathbf{x}) = \sum_{n,m} e^{i(n\mathbf{q}_1+m\mathbf{q}_2)\mathbf{x}}\mathbf{M}_{n\mathbf{q}_1+m\mathbf{q}_2}$ for integers n and m provides the relative weight of $|M_{\mathbf{q}_1+\mathbf{q}_2}|^2/|M_{\mathbf{q}_1}|^2$ and other higher-order peaks.

As shown in Fig. 4(d), all of the experimental findings summarized above are reproduced by this model for typical parameters of MnSi and similar systems [1] including the tiny weight for higher-order peaks and the suppression of the signal around B_{int}. Most importantly, the model shows that the unexpected rise of the higher-order scattering for increasing T (described by increasing t) originates in an overcompensation of the overall drop of the higher-order scattering with increasing T by a shift of B_{int} towards smaller values. Unfortunately, both experimental and theoretical uncertainties, namely, the absolute values of scattering intensities and fluctuation corrections, respectively, prevent a precise quantitative prediction of, e.g., the T dependence of the parameter t. An unresolved issue for future studies concerns the gradual variation of $M_{\mathbf{q}_1}$ for small B [cf. Fig. 4(a)], which may be due to a phase coexistence, while theory predicts a sharp first-order transition [1].

It is finally possible to show that the most prominent feature of both the experiment and the mean-field model, notably the strong suppression of $|M_{\mathbf{q}_1+\mathbf{q}_2}|^2$ around B_{int}, (i) arises from an interference effect and (ii) represents a key property of the Skyrmion lattice. To see this, we note again that almost all of the scattering intensity is given by the six resolution-limited main peaks. The magnetic structure may therefore be approximated very well by a superposition of three helices and the uniform magnetization [1]. Furthermore, a single pair of peaks at $\pm\mathbf{q_i}$ arises from a spin helix of a given chirality [18] determined by the chirality of the atomic structure. A representative of such a helix is $(\Phi\sqrt{2})(0, \sin[qx+\alpha_1], -\cos[qx+\alpha_1])$ or, in Fourier space, $\mathbf{M}_{\mathbf{q}_1} = e^{i\alpha_1}(\Phi/\sqrt{2})(0,-i,-1)$ for $\mathbf{q}_1 = (q,0,0)$, where Φ^2 is the weight of the peak and the phase α_1 describes a shift of the helix. Because the higher-order scattering reported here proves a crystalline character of the magnetic state, it may be constructed in terms of a linear superposition of three such helices rotated by $n2\pi/3$ ($n=0,1,2$) around the z axis. The phases α_i between the helices thereby distinguish the Skyrmion lattice from other (trivial) forms of magnetic order. Two of the three phases may be set to zero in terms of simple translations of the magnetic structure perpendicular to the field. However, the remaining third phase, e.g., $\alpha=\alpha_1$, strongly affects the topological properties of the magnetic structure. In our convention $\alpha=0$ represents the Skyrmion lattice [1]; i.e., in the center of the Skyrmion all three helices point antiparallel to the external magnetic field. Thus knowledge of α allows us to prove microscopically the existence of a Skyrmion lattice in the bulk.

It turns out that no information on α may be inferred from first-order scattering alone, since the signal is sensitive only to $|\mathbf{M}_{\mathbf{q}_i}|^2$. In contrast, the higher-order peaks are very sensitive to the phase α because they are subject to interference effects. Higher-order terms arise from nonlinearities, i.e., from the $\mathbf{M}^4$ term in Eq. (1), as it generates a coupling *linear* in $\mathbf{M}_{\mathbf{q}_1+\mathbf{q}_2}$ arising from $\mathbf{M}_{\mathbf{q}_{1\ldots6}}$ and the uniform magnetization $\mathbf{M}_0$. Collecting all those terms, $\int\mathbf{M}^4 d^3\mathbf{r} = \mathbf{M}_{\mathbf{q}_1+\mathbf{q}_2}\mathbf{b}_{\mathbf{q}_1+\mathbf{q}_2} + \cdots$, one obtains an oscillating effective field $\mathbf{b}_{\mathbf{q}_1+\mathbf{q}_2}$. As $\mathbf{q}_1+\mathbf{q}_2 = 2\mathbf{q}_1+\mathbf{q}_3 = 2\mathbf{q}_2+\mathbf{q}_6$ [see Fig. 2(b)], one finds that the interference of several processes determines the strength of $\mathbf{b}_{\mathbf{q}_1+\mathbf{q}_2}$. Adding all of those terms [examples are $\mathbf{M}_0(\mathbf{M}_{-\mathbf{q}_1}\mathbf{M}_{-\mathbf{q}_2})$ or $\mathbf{M}_{-\mathbf{q}_1}(\mathbf{M}_{-\mathbf{q}_1}\mathbf{M}_{\mathbf{q}_3})$], we obtain

$$\frac{|\mathbf{b}_{\mathbf{q}_1+\mathbf{q}_2}|^2}{2\Phi^6} = 9 + 74\frac{M_0^2}{\Phi^2} - 96\sqrt{2}\frac{M_0}{\Phi}\cos\alpha + 54\cos^2\alpha. \tag{2}$$

A plot of this function for various values of α is shown in Fig. 4(c). Since negative M_0 are unphysical, one finds only for values of α close to $\alpha=0$ that $\mathbf{b}_{\mathbf{q}_1+\mathbf{q}_2}$ becomes very small for a certain magnetic field where $M_0/\Phi = \sqrt{2}24/37 \approx 0.92$ (to be compared to 0.94 and 0.96 obtained from the mean-field theory for $t=-1$ and $t=-5$, respectively). The strong suppression of $\mathbf{M}_{\mathbf{q}_1+\mathbf{q}_2}$ we have observed at B_{int} is therefore the key signature of $\alpha=0$, which microscopically proves the existence of a Skyrmion lattice in bulk samples of MnSi.

We thank E. M. Forgan, P. Granz, M. Janoschek, H. Kolb, M. Laver, J. Peters, B. Russ, R. Schwikowski, D. Wallacher, and A. Zheludev for support and stimulating discussions. T. A. and A. B. acknowledge support through the TUM Graduate School. Financial support through DFG TRR80, SFB608, and FOR960 is gratefully acknowledged.

[1] S. Mühlbauer *et al.*, Science **323**, 915 (2009).
[2] A. Neubauer *et al.*, Phys. Rev. Lett. **102**, 186602 (2009).
[3] W. Münzer *et al.*, Phys. Rev. B **81**, 041203 (2010).
[4] F. Jonietz *et al.*, Science **330**, 1648 (2010).
[5] X. Z. Yu *et al.*, Nature (London) **465**, 901 (2010).
[6] X. Z. Yu *et al.*, Nature Mater. **10**, 106 (2010).
[7] Y. Tokura (personal communication).
[8] Jiadong Zang *et al.*, Phys. Rev. Lett. **107**, 136804 (2011).
[9] M. Janoschek *et al.*, Phys. Rev. B **81**, 214436 (2010).

[10] B. Roessli *et al.*, Phys. Rev. Lett. **88**, 237204 (2002).
[11] F. Semadeni *et al.*, Physica (Amsterdam) **267B–268B**, 248 (1999).
[12] B. Lebech *et al.*, J. Magn. Magn. Mater. **140–144**, 119 (1995).
[13] C. Pfleiderer *et al.*, Phys. Rev. Lett. **99**, 156406 (2007).
[14] G. Shirane, M. Shapiro, and J. Tranquada, *Neutron Scattering with a Triple-Axis Spectrometer—Basic Techniques* (Cambridge University Press, Cambridge, England, 2002).
[15] S. V. Grigoriev *et al.*, Phys. Rev. B **73**, 224440 (2006).
[16] O. Nakanishi *et al.*, Solid State Commun. **35**, 995 (1980).
[17] P. Bak and M. H. Jensen, J. Phys. C **13**, L881 (1980).
[18] M. Tanaka *et al.*, J. Phys. Soc. Jpn. **54**, 2970 (1985).